PCCP

Absolute total electron impact ionization cross-sections for perfluorinated hydrocarbons and small halocarbons

Mark Bart, Peter W. Harland,* James E. Hudson and Claire Vallance†

Department of Chemistry, University of Canterbury, Private Bag 4800, Christchurch, New Zealand. E-mail: p.harland@chem.canterbury.ac.nz

Received 17th November 2000, Accepted 3rd January 2001
First published as an Advance Article on the web 5th February 2001

Absolute total positive-ion electron ionization cross-sections from threshold to 220 eV are reported for a range of halogenated methanes and small perfluorocarbons (2–4 carbon atoms). Correlations between the measured ionization cross-section and related molecular properties, in particular the vertical ionization potential (or vertical appearance energy) and molecular polarizability volume, are noted. Contributions to the total cross-section from individual bonds are also determined. Cross-sections predicted using these 'bond contributions' are in agreement with experiment for a wide range of molecules to better than $\pm 10\%$ accuracy, and in most cases to better than $\pm 5\%$. The experimental data are also compared with ionization efficiency curves calculated using the Deutsch–Märk (DM) and binary encounter Bethe (BEB) models.

1 Introduction

Halocarbons, including perfluorocarbons, are important greenhouse gases. Though chemically inert, they trap more heat per molecule than almost any other gas, and can remain in the atmosphere for up to 50 000 years.[1] They are widely used in the semiconductor industry for cleaning chemical vapour deposition chambers and also have applications as solvents, refrigerants and in fire extinguishers. In the medical sciences, perfluorocarbon liquids have attracted great interest due to their promise as possible blood substitutes for use in surgery and trauma cases,[2–4] and they have also been used in ophthalmic surgery, particularly in the repair of retinal tears (wounds). It is expected that the growing number of applications for these compounds will lead to further concern about their effect on the atmosphere, and a corresponding increase in studies of their gas phase properties. Absolute electron ionization cross-sections are important in the modelling of gas phase systems, in particular for calibrating instruments such as mass spectrometers and ion gauges, which are widely used in experimental studies.

While a number of ionization cross-section measurements have been published for perfluorocarbons and halocarbons, these are limited primarily to studies of CF_4, C_2F_6 and C_3F_8[5] and to the methyl halides.[6] In the present work, measurements are presented for a large range of halogenated methanes and several small-chain perfluorocarbons.

There have been many attempts to model electron ionization efficiency curves. We present comparisons of our experimental data with two of the more successful theories, the DM method of Deutsch and Märk,[7,8] and the binary encounter Bethe model of Kim and Rudd.[9–11] In addition to such *ab initio* and semi-empirical models, several empirical correlations between ionization cross-sections and various molecular properties have been observed. The clear correlation between the electron ionization cross-section and molecular polarisability was explored at some length in an earlier publication;[12] the present results present further support for these observations.

One of the fundamental concepts inherent in many theories of electron ionization is the 'additivity rule', first discovered by Otvos and Stevenson,[13] according to which a molecular ionization cross-section is given by the sum of the cross-sections of individual atoms, or more generally, of atomic orbitals. The rule is based on Bethe's observation[14] that the probability of ionization of an electron in an *n,l* atomic orbital is approximately proportional to the mean-square radius of the orbital. The introduction of bond cross-section contributions to the total ionization cross-section deduced from the measurements reported below, can be rationalised in terms of these same additivity concepts. In relation to the empirical relationship between the maximum ionization cross-section and polarisability volume, this is also consistent with the additive nature of polarisability contributions to the overall molecular polarisability.

In a variation on the additivity rule, Bobeldijk *et al.*[15] determined a set of bond contributions to the photoionization cross-sections of hydrocarbons and oxygen-containing organic molecules. The contributions were determined from experimental and semi-empirical data, and were found to be in agreement with experiment to within about $\pm 20\%$. In the present work, we present a similar set of bond contributions for electron-impact ionization cross-sections. Simple addition of these bond contributions predicts cross-sections in very close agreement with experiment for a wide range of molecular systems.

2 Experimental

The ionization cell used for these measurements, which is a modified version of the condenser plate ion source used by Tate and Smith,[16] has been described previously.[6] The ionization cell is housed in a vacuum chamber with a typical background pressure of $\sim 10^{-7}$ Torr. Electrons are emitted from a resistively heated rhenium filament which is biased at a potential that determines the electron energy. A shield held at a negative potential of 2 V with respect to the filament serves to

† Present address: Physical and Theoretical Chemistry Laboratory, Oxford University, Oxford, UK OX1 3QZ.

 DOI: 10.1039/b009243f

repel the electrons towards a set of three stainless steel electrostatic lens elements which collimate the electron beam and focus it into the cylindrical collision cell. The walls of the collision cell are coated with colloidal graphite to prevent surface scattering of charged particles, an important consideration since the cell walls also serve as the ion collector. Sample gas is admitted to the collision cell using a Leybold-Heraeus needle valve into a 3 mm inlet drilled in the cell wall, allowing fine control of the flow rate. A second 3 mm aperture in the cell wall connects the cell to an MKS Type 627A, 0.05 Torr full scale Baratron capacitance manometer. The gas sample is assumed to be in thermal equilibrium with the walls of the collision cell, and a thermistor in contact with the outer wall of the cell is used to measure the gas temperature. After traversing the collision cell, the electron beam passes through two further lens elements before collection on a Faraday plate. The ion current from the collision cell wall and electron current from the Faraday plate are recorded using Keithley Model 486 picoammeters.

Absolute electron ionization cross-sections, σ_i, can be calculated from

$$\frac{I^+}{I^-} = n\sigma_i x \quad (1)$$

where I^+ and I^- are the measured ion and electron currents, n is the number density of the target gas, and x is the path length through the collision cell. Assuming ideal gas behaviour,

$$n = \frac{P}{k_B T} \quad (2)$$

where P and T are the pressure and temperature of the target gas and k_B is Boltzmann's constant.

In a typical experiment, the pressure of the sample gas is maintained at about 3×10^{-4} Torr. The electron current is kept below 100 nA in order to preclude space-charge effects. Typical ion currents are in the range 0.1 to 10 nA. The picoammeters used to record the electron and ion currents are computer interfaced through an IEEE parallel bus, while the analog signals from the thermistor and capacitance manometer (after amplification) are passed to the computer through a commercial 14-bit I/O card. The I/O card is also used to program the electron energy using a Spellman Model MS0.3N, 0 to −300 V, computer-controllable power supply. At each experimental point, the electron energy is set and a temperature reading is taken. The ion and electron currents and the target gas pressure are taken as the average of ten, one second readings at each electron energy. Reproducibility from run to run, even measured weeks apart, is very good. The ionization efficiency curves reported here are the average of between five and ten repeated determinations made over a period of several months. We have previously determined the accuracy of cross-sections measured using this instrument to be 4% or better.[12]

3 Calculations

While electron ionization is essentially a quantum mechanical process, it is too complicated to carry out comprehensive quantum mechanical calculations on any but the simplest atomic systems, largely because the exit channel of the encounter constitutes a complicated three-body problem. This has led to the development of a range of semi-empirical and semi-classical models for predicting ionization efficiency curves.[16] Two widely used methods are the binary encounter Bethe (BEB) model, developed by Kim and Rudd,[9–11] and the additivity model developed by Deutsch and Märk (DM).[7,8] The experimental results reported in this paper have been compared with the predictions of these two models, and also with the predictions of a simple electrostatic model based on the observed correlation between the absolute electron ionization cross-section and the molecular polarisability volume.[12]

The BEB model, based on the earlier binary encounter dipole theory by the same authors, uses a combination of Mott scattering theory augmented by binary encounter theory for low energy collisions, and the Bethe theory for high energy collisions. In order to apply the BEB theory it is necessary to determine the orbital occupation number N, average orbital kinetic energy U, and orbital binding energy B for each molecular orbital. In this work the molecular orbital package GAMESS[17] was used to calculate these properties. The electron ionization cross-section for each orbital is given by

$$\sigma_{BEB} = \frac{S}{t+u+1}\left[\frac{\ln(t)}{2}\left(1-\frac{1}{t^2}\right)+1-\frac{1}{t}-\frac{\ln(t)}{t+1}\right] \quad (3)$$

where $t = T/B$ is the reduced incident electron energy at incident electron energy T, $u = U/B$ is the reduced orbital kinetic energy; and $S = (4\pi a_0^2 N R^2)/B^2$, in which $R = 13.6$ eV is the ionization potential of the hydrogen 1s orbital, and a_0 is the Bohr radius.

The total molecular cross-section is found by summing over the occupied orbitals. As suggested by Kim,[18] in order to improve the empirical accuracy of the theory, whenever an atomic orbital with principle quantum number n greater than two dominates the molecular orbital, the kinetic energy of the orbital is divided by n in the summation.

The Deutsch–Märk model has its origins in a model proposed by J. J. Thomson in 1912. Thomson's original model has been improved in various ways over the years; Deutsch and Märk's contribution was to integrate the resulting theory with the theory developed by Bethe, and to use Otvos and Stevenson's additivity rule to extend the domain of the calculations from atomic to molecular ionization cross-sections. The DM cross-section is given by

$$\sigma_{DM} = \sum_{i;\,nl} \pi r^2_{i;\,nl} \sum_j g^j_{i;\,nk} N^j_{i;\,nl} f(u_j) \quad (4)$$

where $u_j = T/B_j$ (the electron energy divided by the molecular orbital energy); $r^2_{i;\,nl}$ is the mean square radius of the n,l atomic shell on atom i; $N^j_{i;\,nl}$ is the population of atomic orbital i in molecular orbital j (from a Mulliken analysis); $g^j_{i;\,nl}$

Table 1 Experimental and calculated (BEB and DM) maximum total ionization cross-sections for small mixed halocarbons and nitriles and a series of perfluorocarbons, expressed in units of Å^2 (1 Å^2 = 1×10^{-20} m^2). The percentage differences between calculated and experimental values are shown in parentheses

Molecule	σ_{max}(exptl)	σ_{max}(BEB)	σ_{max}(DM)
CF_4	4.75	4.89(+2.9)	4.97(+4.7)
C_2F_4	5.90	6.38(+8.1)	7.19(+21.9)
C_2F_6	7.64	7.85(+2.7)	11.46(+50.0)
CF_3CFCF_2	8.83	9.62(+8.9)	10.69(+21.1)
C_3F_8	10.33	11.42(+10.6)	12.11(+17.2)
CF_3CCCF_3	10.27	10.43(+1.6)	13.51(+31.5)
$CF_2CFCFCF_2$	10.46	10.70(+2.3)	13.02(+24.5)
$CF_3CFCFCF_3$	11.60	11.90(+2.6)	15.79(+36.1)
CH_3F	3.78	3.64(−3.7)	4.99(+32.0)
CF_3H	4.32	4.53(+4.9)	5.69(+31.7)
CF_2Cl_2	9.57	7.23(−24.5)	9.84(+2.8)
CF_3Cl	6.93	6.65(−4.0)	8.30(+19.8)
CF_3Br	7.87	6.72(−14.6)	7.99(+1.5)
CF_3CN	6.33	7.45(+17.7)	7.69(+21.5)
CH_3CN	6.33	5.60(−11.5)	7.90(+24.8)
CCl_3CN	14.11	—	—
CF_2Br_2	—	8.42	11.29
CH_2Br_2	11.67	7.76(−33.5)	—
$CHBr_3$	13.75	9.86(−28.3)	14.78(+7.5)
CBr_4	19.0	—	—
SF_6	7.10	7.33(+3.2)	9.67(+36.2)

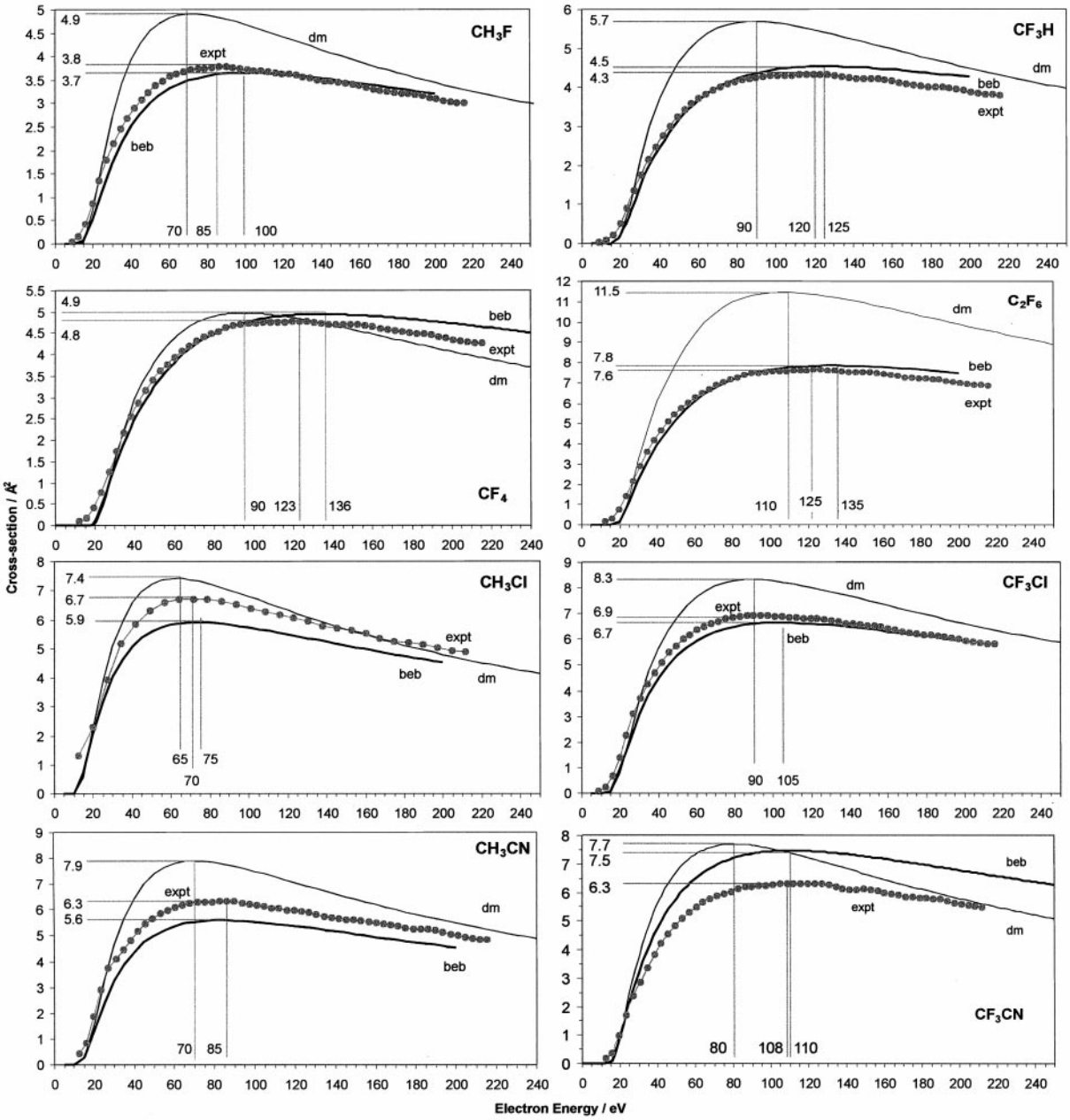

Fig. 1 Calculated and experimentally measured total ionization efficiency curves for the halocarbons and nitriles: CH_3F; CF_3H; CF_4; C_2F_6; CH_3Cl; CF_3Cl; CH_3CN; CF_3CN. The maximum total ionization cross-sections and the corresponding electron energies are marked on the plots.

are empirically determined weighting factors; and

$$f(u) = \frac{1}{u}\left(\frac{u-1}{u+1}\right)^{3/2} \times \left(1 + \frac{2}{3}\left(1 - \frac{1}{2u}\right)\ln[2.7 + (u-1)^{1/2}]\right) \quad (5)$$

The electrostatic model of the ionization process described by Harland and Vallance[12] relates the maximum total ionization cross-section, σ_{max}, to the molecular properties volume polarisability, α, and vertical ionization potential, E_0, given by eqn. (6),

$$\sigma_{max} = c'\left(\frac{\alpha}{E_0}\right)^{1/2} \quad (6)$$

where c' is a constant. Although eqn. (6) was derived from first principles, the empirical correlation in eqn. (7) between maximum electron ionization cross-section and polarisability, where c is a constant, discussed in ref. 12, is also very good.

$$\sigma_{max} = c\alpha \quad (7)$$

4 Results and discussion

4.1 Experimental data

Experimentally determined maximum cross-sections, DM and BEB maximum cross-sections and their percentage deviations from experiment are presented in Table 1. The only molecules listed for which ionization cross-section data have been reported previously in the literature are SF_6, CF_4, C_2F_6 and C_3F_8. Ionization efficiency curves for these molecules can be found in the BEB database on the NIST website.[5] Rapp and Englander-Golden[19] reported a value of 7.0 Å^2 for the maximum cross-section for SF_6 and 3.64 Å^2 for CF_4, compared with the values of 7.10 and 4.75 Å^2 shown in Table 1. Although Rapp and Englander-Golden's data for SF_6 appear in the BEB database, their data for CF_4 have not been included; maximum cross-sections for CF_4 included in the database range from 5.2 to 6.1 Å^2. Experimental data shown for C_2F_6 exhibit values of the maximum cross-section over the range from 8.0 to 10.0 Å^2, compared with our measurement of 7.64 Å^2. Reported maximum cross-sections for C_3F_8 range from 7.5 to 17.5 Å^2, compared with our measured value of

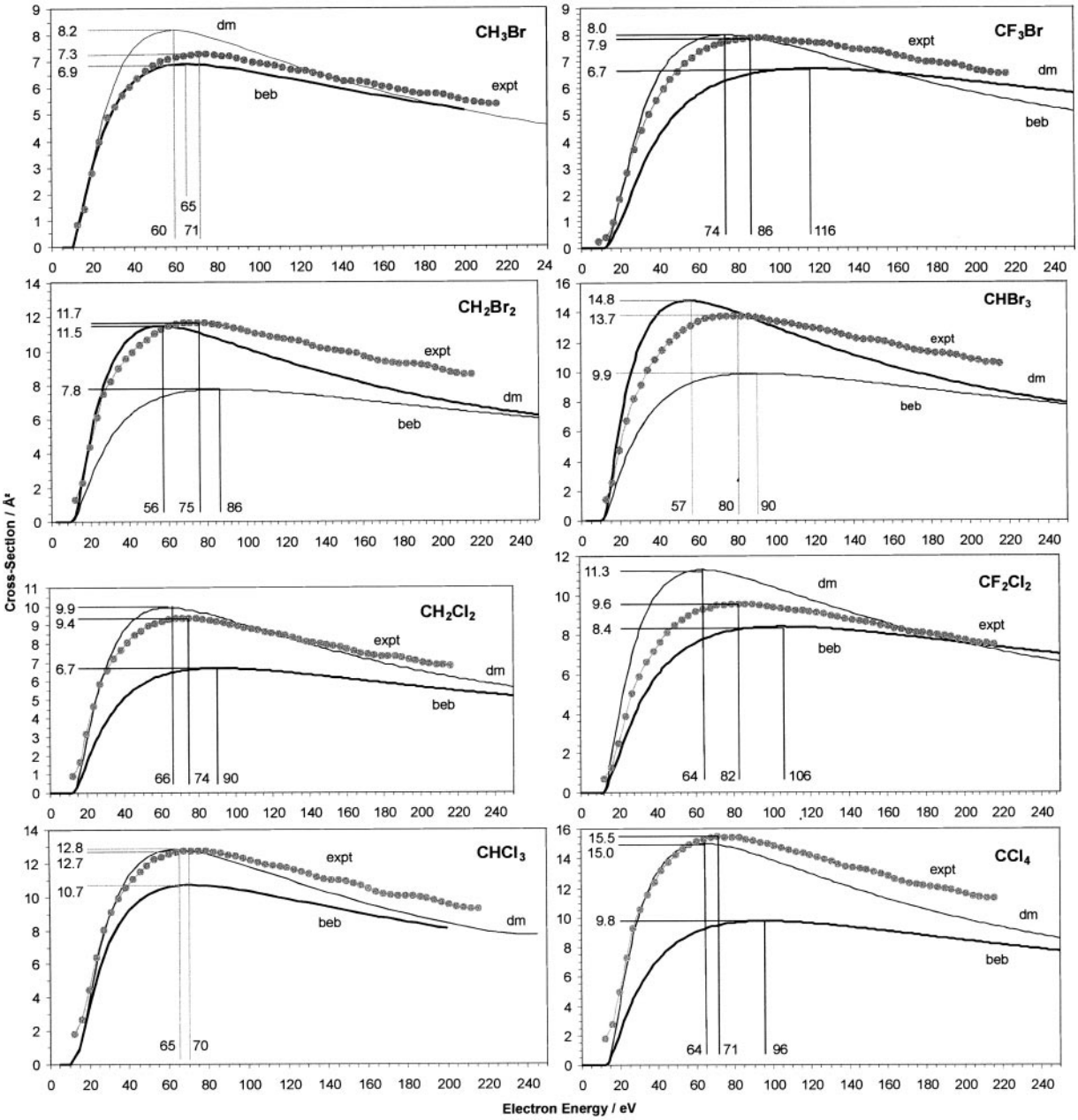

Fig. 2 Calculated and experimentally measured total ionization efficiency curves for the halocarbons: CH_3Br; CF_3Br; CH_2Br_2; $CHBr_3$; CH_2Cl_2; CF_2Cl_2; $CHCl_3$; CCl_4. The maximum total ionization cross-sections and the corresponding electron energies are marked on the plots.

10.33 Å^2. There is clearly a wide distribution of measured values for absolute total ionization cross-sections, even for relatively small, 'simple' molecules.

4.2 Model calculations

In Fig. 1 and 2, the experimentally measured ionization efficiency curves for a selection of the molecules studied are compared with the DM and BEB calculations; in each case the maximum in the cross-section and the corresponding electron energy are marked. We have shown previously[12] that the best choice of theoretical model depends on the molecule under study; these conclusions are reinforced by the present work. Fig. 1 and 2 show that the DM calculations generally overestimate the ionization cross-section and typically underestimate the electron energy at the maximum by about 15–20 eV, though it is interesting to note that for molecules containing bromine or more than one chlorine atom, the model performs significantly better. In contrast, the BEB calculations are in close agreement with the experimental measurements for small, non-bromine containing molecules. The model more-or-less correctly reproduces experimental ionization efficiency curves for the full range of molecules studied, although the predicted electron energies corresponding to the maxima are higher than the measured values, typically by around 10–15 eV.

Fig. 3 shows experimental curves for the perfluorocarbons studied. Again, BEB calculations are generally in good agreement with experiment, with moderate differences in the maximum cross-section and corresponding electron energy E_{max}. Disparities for the DM calculations are significantly larger, with maximum cross-sections overestimated by 20% or more (up to 50% in some cases) and E_{max} displaced to lower energy by 10–20 eV. The performance of the DM model for these molecules appears to be consistent with a recent study of the C_2F_5 radical by Tarnovsky and coworkers.[20] Their DM calculation of the ionization efficiency curve for total ionization resulted in a maximum cross-section around 20% higher than the experimentally measured value.

Several trends emerge when the discrepancies between theory and experiment are investigated in more detail. Fig. 4 is a plot of BEB (triangles) and DM (squares) calculated

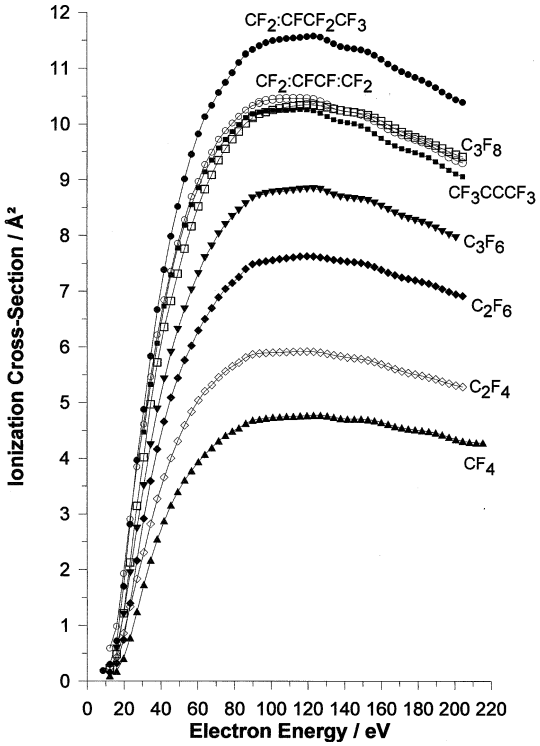

Fig. 3 Experimentally measured ionization efficiency curves for the C_1 to C_4 perfluorocarbons: CF_4; C_2F_4; C_2F_6; C_3F_6; C_3F_8; C_4F_6-2-yne; C_4F_6-1,3-diene; C_4F_8-1-ene.

maximum cross-sections against experimental measurements from this work and from a previous publication.[6] The narrow line represents the experimental data and the heavy lines are linear least-squares fits forced through the origin for the BEB and DM cross-section data sets. With the exception of three molecules, CO_2 (−29.1%), CCl_4 (−2.9%) and CH_2Br_2 (−3.3%), the cross-sections calculated using the DM model are higher than those measured, as illustrated in the deviation plot in Fig. 4. For the BEB calculations, perfluorocarbons give positive deviations, while negative deviations are obtained for molecules containing chlorine, bromine or the nitrile group. It is possible that some of the inconsistencies between theory and experiment for molecules containing heavy atoms are due to the level of theory at which the *ab initio* calculations were carried out in the determination of the required molecular orbital properties. Due to the size of some of the molecules studied, high level calculations were not possible in many cases, and for consistency, all calculations were carried out at a similar level of theory, namely HF/6-31G for all molecules apart from brominated halocarbons, for which HF/3-21G was used. While the following may not necessarily hold true for larger molecules containing heavy atoms, a series of calculations for CF_4 using different basis sets and levels of theory showed only a small variation in the resulting DM and BEB cross-sections.

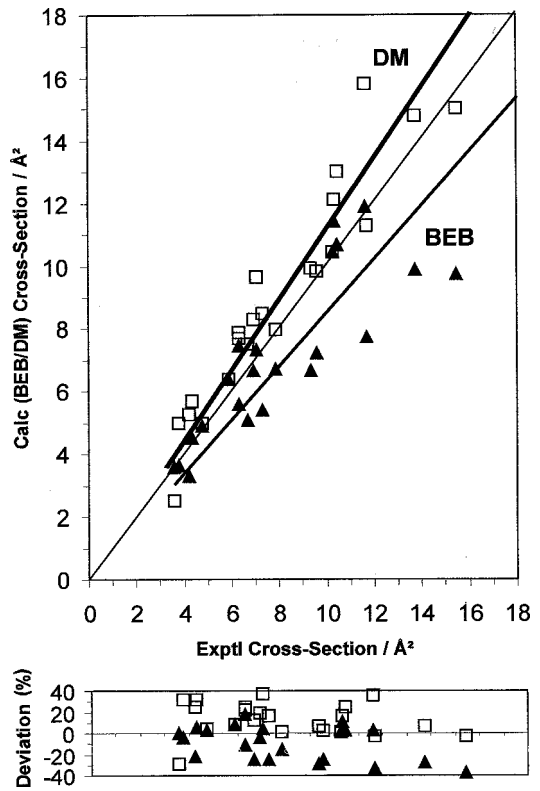

Fig. 4 Plot of the BEB (closed triangles) and DM (open squares) calculated maximum total ionization cross-sections against the experimentally measured values for the molecules in Table 1 and those reported previously in ref. 6. The difference plot shows the percentage deviation of the calculated values from the measured values.

4.3 Correlation with molecular parameters

In an earlier paper on the relationship between electron ionization cross-section and the molecular electrostatic parameters,[12] it was found that there is a clear linear relationship between the maximum cross-section σ_{max} and both the molecular polarisability volume α and the quantity $(\alpha/E_0)^{1/2}$, in which E_0 is the ionization potential for production of the molecular ion. The observations were based on an analysis of all reported ionization cross-section data for atoms and molecules ranging in size from H_2 to $C_{10}H_{22}$, including our own experimental measurements, and could be summarised in a set of simple relationships.

$$\sigma_{max} = 1.418\alpha + 0.310 \quad (R^2 = 0.969) \tag{8}$$

$$\sigma_{max} = 1.455\alpha, \text{ forced through the origin} \quad (R^2 = 0.989) \tag{9}$$

and

$$\sigma_{max} = 17.97\left(\frac{\alpha}{E_0}\right)^{1/2} - 4.14 \quad (R^2 = 0.945). \tag{10}$$

In the above expressions, α has units of Å^3 (10^{-24} cm^3), E_0 is in eV and σ_{max} is in Å^2. The new results reported here simply reinforce the observed correlations, as shown in Fig. 5 and 6.

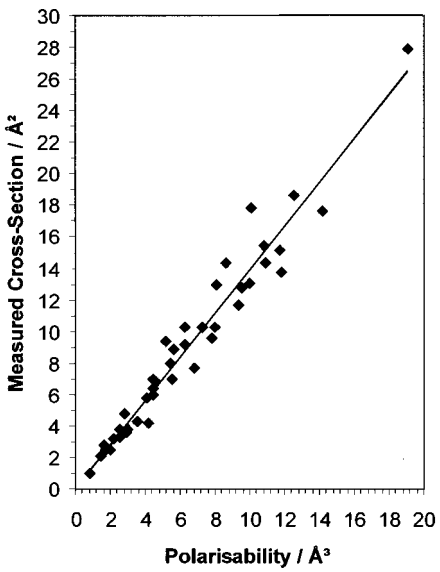

Fig. 5 Plot of experimentally measured maximum total ionization cross-section (Table 1, ref. 5, 6, 15 and 19) against polarisability volume.

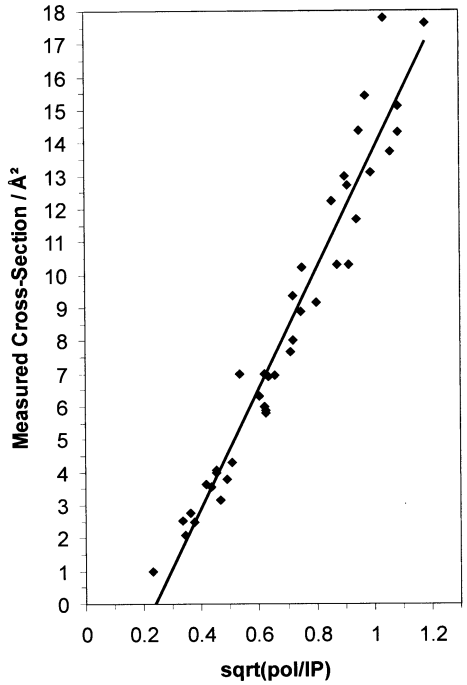

Fig. 6 Plot of experimentally measured maximum total ionization cross-section (Table 1, ref. 5, 6, 15 and 19) against the square root of the ratio of polarisability volume to ionization potential.

Note that some of the point scatter in these plots results from the spread in available literature values of the molecular polarisability and/or absolute maximum ionization cross-section for a number of the molecules studied.[21] Inclusion of the new data does not greatly affect either the numerical constants in the empirical expressions, or the variance of the least squares fit. The refined expressions for the maximum ionization cross-sections are as follows:

$$\sigma_{max} = 1.378\alpha + 0.153 \quad (R^2 = 0.955) \qquad (11)$$

$$\sigma_{max} = 1.395\alpha, \text{ forced through the origin} \quad (R^2 = 0.955) \qquad (12)$$

and

$$\sigma_{max} = 18.13\left(\frac{\alpha}{E_0}\right)^{1/2} - 4.34 \quad (R^2 = 0.947). \qquad (13)$$

Plots of the BEB and DM σ_{max} values against volume polarisability show greater scatter than the corresponding plot for the experimental data, with least-squares fits giving a variance of 0.813 for the BEB data and 0.929 for the DM results.

Using the experimental cross-sections shown in Table 1 and reported in ref. 12, the contributions of individual bonds to the maximum molecular ionization cross-section have been determined. These are shown in Table 2. Using these data, the maximum total ionization cross-section for a molecule is estimated by simply adding the contributions from each bond. For example, the cross-section for CCl_3CN, which cannot be calculated readily using the BEB or DM models, is given by the sum 3(C–Cl) + (C–CN), yielding an estimate of 14.4 Å², compared with the measured value of 14.1 Å². For n-C_6H_{14}, summation of bond contributions, 5(C–C) + 14(C–H), gives a cross-section of 19.0 Å², compared with a literature value[15] of 17.8 Å². The estimated value for the perfluorocarbon C_4F_6 isomer CF_2=CFCF=CF_2 is 10.6 Å², *i.e.* (C–C) + 2(C=C) + 6(C–F), compared with the measured value of 10.5 Å². These encouraging results are borne out by a more extensive comparison with the available data. Fig. 7 shows a plot of the maximum electron-impact ionization cross-sections determined by adding the bond contributions in Table 2 against experimental values for the complete set of available data used in Fig. 5 and 6. All of the experimental cross-sections are reproduced to within 10% and most to within 5%.

The reliability of this approach for every molecule to which it has been applied lends a great deal of confidence to using it for the prediction of as-yet unmeasured ionization cross-sections. Recently,[22] we received a request for measurements of the maximum cross-sections for CF_2Br_2 and $(CF_2Br)_2$. BEB and DM calculations for these molecules are shown in Fig. 8; for $C_2F_4Br_2$, the DM model predicts 14.5 Å² and the BEB model 12.2 Å², while for CF_2Br_2, the DM model predicts 11.3 Å² and the BEB model 8.4 Å². Based on the previous comparisons with experiment for similar brominated molecules, such as CF_3Br and CH_2Br_2, we may expect that the DM result is more accurate in these cases. We cannot use the empirical relationships of eqn. (11)–(13) as a check, since the polarisability for CF_2Br_2 is not known accurately[22] and there is no literature value for $C_2F_4Br_2$. Using the bond contribution approach, we can estimate the cross-sections to be 11.2 and 14.4 Å² respectively for CF_2Br_2 and $(CF_2Br)_2$, with a high degree of confidence that these values lie within at least

Table 2 Additive bond contributions to molecular maximum ionization cross-section

Bond	Cross-section component/Å²
C–H	1.0
C–F	1.1
C–Cl	3.8
C–Br	4.5
C–I	7.3
C–CN	3.0
C–C	1.0
C=C	1.5
C≡C	1.7

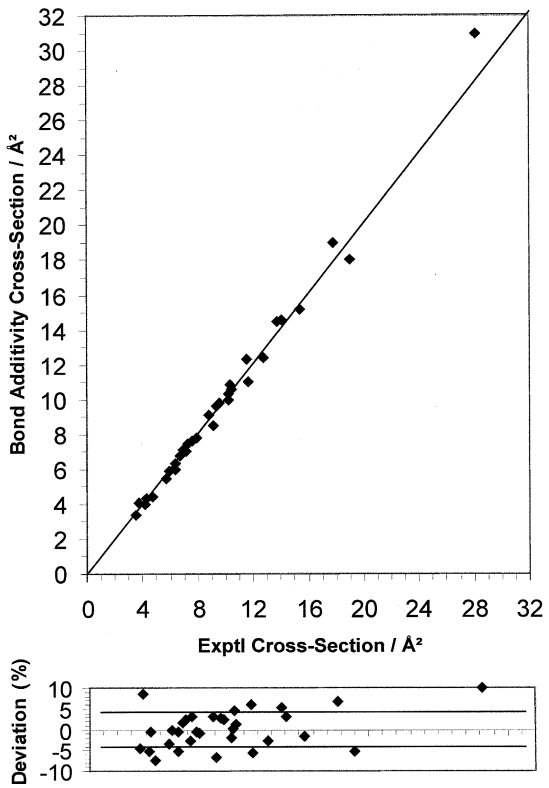

Fig. 7 Plot of the cross-sections determined from the bond additivity values shown in Table 2 against the experimental values for the molecules plotted in Fig. 5 and 6. The difference plot shows the percentage deviation of the estimated values from the measured values.

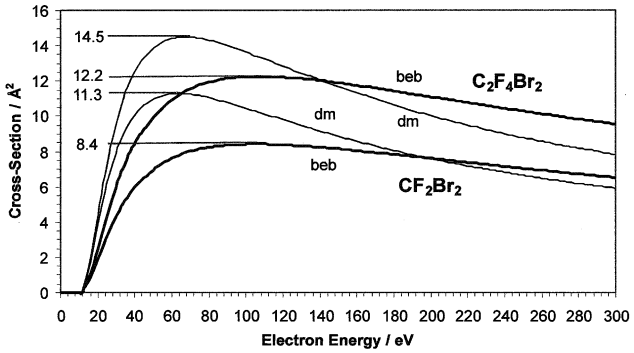

Fig. 8 Calculated BEB (thick lines) and DM (thin lines) total ionization efficiency curves for CF_2Br_2 and $C_2F_4Br_2$. The maximum total ionization cross-sections and the corresponding electron energies are marked on the plots.

5–10% of the measured value. These values are in reassuringly close agreement with the DM results. Unfortunately, we are unable to obtain samples of these compounds[23] to carry out an experimental determination of their ionization cross-sections. In practice, the trends observed in the comparisons of DM and BEB model curves together with experiment for similar molecules can be used to advantage. The shape of the experimental curves is fairly closely matched by the DM data below the maximum, then tends to lie between the two theoretical curves as the electron energy is increased, the bond additivity and model cross-section data could be used to construct useful ionization efficiency curves for molecules where experimental data are unavailable.

5 Conclusion

In addition to the examples given in the Introduction and the text, absolute ionization cross-sections are required for many research applications. In our case, we have an interest in collisions between electrons and spatially oriented molecules.[24] Only relative cross-sections can be measured in the crossed beams experiment and we rely on the absolute values measured in the collision cell or available in the literature. These same considerations apply to many other areas of ion chemistry and physics such as the two-dimensional time-of-flight mass spectrometry studies of multiply charged ion formation and dissociation, where relative cross-sections are determined.[25]

The ionization cross-sections reported in this study account for a significant fraction of the total absolute ionization cross-sections in the literature. Three equations based on our electrostatic model of the ionization process[12] are presented for the estimation of unknown maximum ionization cross-sections. Eqn. (11) and (12) may be used to estimate cross-sections where the molecular polarisability volumes are available, Fig. 5 and 7. In cases where there is a molecular ion, the polarisation volume and the ionization potential can be used in eqn. (13) to estimate a cross-section with a higher degree of confidence than eqn. (11) or (12). The bond additivity cross-sections listed in Table 2, developed from our measured values and values taken from the literature, can be used to estimate unknown cross-sections with a high level of confidence, Fig. 7. Significant differences between the cross-sections of the two isomeric C_4F_6 perfluorocarbons have been attributed to the different additivity contributions of the carbon–carbon double and triple bonds. The strengths and weaknesses of the DM and BEB calculated ionization efficiency curves for the molecules studied should help to direct researchers to the best method for their molecule of interest. In addition, the shapes of the experimental and calculated curves for the wide range of molecules now studied will allow the estimated maximum cross-section for an unknown molecule to be fitted to an ionization curve of reasonable shape.

6 Acknowledgements

PWH should like to acknowledge the Marsden Fund for support of this work through grant 99-UOC-032 PSE.

References

1 *Climate Change 1995—The Science of Climate Change*, ed. J. T. Houghton, L. G. Meira Filho, B. A. Callander, N. Harris, A. Kattenburg and K. Maskell, Cambridge University Press, Cambridge, 1996.
2 R. P. Geyer, *Biomater. Artif. Cells, Artif. Organs*, 1988, **16**, 31.
3 K. C. Lowe, *Chem. Ind.*, 1991, **4 Feb**, 83.
4 R. K. Spence, *Artif. Cells, Blood Substitutes, Immobilization Biotechnol.*, 1995, **23**, 367.
5 See BEB database at http://physics.nist.gov/cgi-bin/Ionization/
6 C. Vallance, S. A. Harris, J. E. Hudson and P. W. Harland, *J. Phys. B*, 1997, **30**, 2465.
7 D. Margreiter, H. Deutsch and T. D. Märk, *Contrib. Plasma Phys.*, 1990, **30**, 487.
8 D. Margreiter, H. Deutsch and T. D. Märk, *Int. J. Mass Spectrom. Ion Processes*, 1994, **139**, 127.
9 Y. K. Kim and M. E. Rudd, *Phys. Rev. A*, 1994, **50**, 3954.
10 W. Hwang, Y. K. Lim and M. E. Rudd, *J. Chem. Phys.*, 1996, **104**, 2956.
11 Y. K. Kim, W. Hwang, N. M. Weinberger, M. A. Ali and M. E. Rudd, *J. Chem. Phys.*, 1997, **106**, 1026.
12 P. W. Harland and C. Vallance, *Int. J. Mass Spectrom. Ion Processes*, 1997, **171**, 173.
13 J. W. Otvos and D. P. Stevenson, *J. Am. Chem. Soc.*, 1956, **78**, 546.
14 H. Bethe, *Ann. Phys.* (*Leipzig*), 1930, **5**, 325.
15 M. Bobeldijk, W. J. Van der Zande and P. G. Kistemaker, *Chem. Phys.*, 1994, **179**, 125.
16 P. W. Harland and C. Vallance, in *Advances in Gas-Phase Ion Chemistry*, ed. N. G. Adams and L. M. Babcock, JAI Press Ltd., London, 1998, vol. 3.
17 M. W. Schmidt, K. K. Baldridge, J. A. Boatz, S. T. Elbert, M. S. Gordon, J. H. Jensen, S. Koseki, N. Matsunaga, K. A. Nguyen, S. J. Su, T. L. Windus, M. Dupuis and J. A. Montgomery, *J. Comput. Chem.*, 1993, **14**, 1347.
18 Y. K. Kim *et al.*, personal communication, 1999.
19 D. Rapp and P. Englander-Golden, *J. Chem. Phys.*, 1965, **43**, 1464.
20 V. Tarnovsky, H. Deutsch and K. Becker, *J. Phys. B*, 2000, **32**, L573.
21 *Handbook of Chemistry and Physics*, ed. D. R. Lide, CRC Press, Boca Raton, FL, 73rd edn., 1992–1993.
22 M. J. Dorko, personal communication, Michigan State University, 2000.
23 The New Zealand Government introduced the "The Ozone Layer Protection Order 1991" which prohibits the importation of a large number of named halocarbons, including CF_2Br_2 and $(CF_3Br)_2$, even for research purposes. The halocarbons used in this study were purchased pre-1991.
24 For example: C. G. Aitken, D. A. Blunt and P. W. Harland, *Int. J. Mass Spectrom. Ion Processes*, 1995, **149/150**, 279; P. R. Brooks and P. W. Harland, in *Advances in Gas Phase Ion Chemistry*, ed. N. G. Adams and L. M. Babcock, JAI Press Inc., London, 1996, vol. 2.
25 See for example, P. Calandra, C. S. S. O'Connor and S. D. Price, *J. Chem. Phys.*, 2000, **112**, 10821, and references therein.